Air-sea CO_2 fluxes for the Brazilian northeast continental shelf in a climatic transition region

CrossMark

A.C.O. Carvalho [a], R.V. Marins [a,*], F.J.S. Dias [b], C.E. Rezende [e], N. Lefèvre [c], M.S. Cavalcante [a], S.A. Eschrique [d]

[a] Laboratório de Biogeoquímica Costeira, Instituto de Ciências do Mar, Universidade Federal do Ceará (LBC/LABOMAR/UFC), Fortaleza, Ceará, Brazil
[b] Laboratório de Hidrodinâmica Costeira, Estuarina e Águas Interiores, Universidade Federal do Maranhão (LHiCEAI/UFMA), São Luiz, Maranhão, Brazil
[c] Laboratoire d'océanographie et du climat: expérimentations et approches numériques - (LOCEAN), Institut de recherche pour le développement (IRD), Paris, France
[d] Laboratório de Biogeociclos dos Constituintes Químicos da Água, Universidade Federal do Maranhão (LABCICLOS/UFMA), São Luiz, Maranhão, Brazil
[e] Laboratório de Ciências Ambientais, Centro de Biociências e Biotecnologia, Universidade Estadual do Norte Fluminense Darcy Ribeiro, Av. Alberto Lamego, 2000, 28013-602 Campos dos Goytacazes – RJ, Brasil

ARTICLE INFO

ABSTRACT

Oceanographic cruises were carried out in October 2012 (3°S–5°S and 38,5°W–35,5°W) and in September 2014 (1°S–4°S and 43°W–37°W), measuring atmospheric and sea surface CO_2 fugacity (fCO_2) underway in the northeast coast of Brazil. Sea surface water samples were also collected for chlorophyll a, nutrients and DOC analysis. During the second cruise, the sampling area covered a transition between semi-arid to more humid areas of the coast, with different hydrologic and rainfall regimes. The seawater fCO_2^{sw}, in October 2012, was in average 400.9 ± 7.3 μatm and 391.1 ± 6.3 μatm in September 2014. For the atmosphere, the fCO_2^{air} in October 2012 was 375.8 ± 2.0 μatm and in September 2014, 368.9 ± 2.2 μatm. The super-saturation of the seawater in relation to the atmosphere indicates a source of CO_2 to the atmosphere. The entire study area presents oligotrophic conditions. Despite the low concentrations, Chl a and nutrients presented significant influence on fCO_2^{sw}, particularly in the westernmost and more humid part of the northeast coast, where river fluxes are three orders of magnitude larger than eastern rivers and rainfall events are more intense and constant. fCO_2^{sw} spatial distribution presented homogeneity along the same transect and longitudinal heterogeneity, between east and west, reinforcing the hypothesis of transition between two regions of different behaviour. The fCO_2^{sw} at the eastern portion was controlled by parameters such as temperature and salinity. At the western portion, fCO_2^{sw} was influenced by nutrient and Chl a. Calculated instantaneous CO_2 flux ranged from $+1.66$ to $+7.24$ mmol m^{-2} d^{-1} in the first cruise and $+0.89$ to $+14.62$ mmol m^{-2} d^{-1} in the second cruise.

© 2017 Elsevier B.V. All rights reserved.

1. Introduction

Anthropogenic CO_2 emissions to the atmosphere are increasing at a steady rate. The ocean and the terrestrial biosphere absorb a great part of these emissions (Sabine et al., 2004; Canadell et al., 2007). Robust CO_2 climatology (Takahashi et al., 2002; Takahashi et al., 2009) reveals a heterogeneous behaviour, with higher latitudes acting as a sink of CO_2 and lower latitudes acting as a source of CO_2 to the atmosphere. However, the ocean margins are not computed in this analysis and the role of the costal oceans is not well elucidated. There is a debate about coastal CO_2 distribution (Bauer et al., 2013) and many studies suggest the importance of these regions in carbon budgets and CO_2 fluxes (Tsunogai et al., 1999; Cai et al., 2006; Laruelle et al., 2010; Laruelle et al., 2014; Gruber, 2015).

The coastal waters represent a link between terrestrial and oceanic systems, receiving large amount of continental material through river discharges and groundwater, as well as by exchanges between the atmosphere, sediments and the open ocean. Though it represents a small portion of the total oceanic area, it consists in a major contribution to the global carbon cycle and thus, should not be ignored in the carbon budgets (Borges et al., 2005; Chen and Borges, 2009).

Continental margins tend to show greater space and time variability than most remote regions in the oceans and receive more pressure from human activities. Land use and water resources can also alter coastal systems significantly (Jiang et al., 2013). However, coastal oceans are often misrepresented in the global carbon balance. Many studies, however, have shown interest for these areas and their carbon transfer mechanisms in the ocean-atmosphere interface, which has helped to understand the role of continental margins in the CO_2 fluxes (Chen et al., 2013 and references therein).

There are many studies in the temperate systems and only a few studies in tropical ones. Previous measurements in the tropical Atlantic

* Corresponding author.
E-mail address: rmarins@ufc.br (R.V. Marins).

concluded that it is generally a source of CO_2 to the atmosphere (Andrié et al., 1986; Goyet et al., 1998). Some of its regions represent CO_2 sinks due to the Amazon River discharge causing strong biological activity and CO_2 uptake (Ternon et al., 2000; Körtzinger, 2003; Cooley and Yager, 2006; Ibánhez et al., 2016).

Earlier studies have reported few measurements conducted in the coastal zone and more specifically at the Brazilian coast. The scarcity of estimates of air-sea CO_2 fluxes in regions of the Brazilian continental shelf and the need to understand the effects of climate change on carbon cycle has led to great efforts to measure fCO_2. During the 'Ocean Circulation in the Southwest Atlantic Region' program (COROAS), fCO_2 measurements performed in the Brazilian Southwest region contributed to a better understanding of the role of continental shelf in the ocean carbon cycle (Ito et al., 2005).

In this study, fCO_2 underway measurements were made in the Brazilian Equatorial Northeastern coastal zone from about 5°S to 0°S, as an effort to contribute with oceanographic cruises performed to better understand the fCO_2 variability in this region.

2. The study area

This study concerns the Brazilian Equatorial Northeast continental shelf (Fig. 1), which is narrow, open to the ocean and oligotrophic. In the Northeast of Brazil, semi-arid climate has led to the building of dams, reducing continental run-off and therefore, inputs for the primary productivity in the coastal ocean.

The rainy season usually extends from January to June and the months of July to December mark the dry season. Monthly mean rainfall values (mm) for the years of 2012 and 2014 were below the expected for the period, when compared to the historical mean for the years of (2000 − 2010) showing a tendency of prolonged drought. Regional rivers such as the Jaguaribe, the Parnaíba and the rivers contributors to São Marcos Bay (SMB) are strongly influenced by climatic seasonality. Average annual rainfall for the Jaguaribe and Parnaíba rivers are respectively: 80 and 91.6 mm. The Parnaíba basin characterizes a transition between the Brazilian northeastern semi-arid region, with intermittent

rivers, and the Amazon, where high rainfall and perennial rivers prevail. For the SMB region, this average is about two times higher, 191.3 mm, representing a more humid coastal area. (Fig. 2).

Trade winds from the SE dominate during the dry season, when wind speed is maximum and associated with the lowest temperature, when this study was performed.

Assessments developed by REVIZEE ('Avaliação do Potencial Sustentável de Recursos Vivos na Zona Econômica Exclusiva') and JOPS-II ('Brazil-German Joint Oceanographic Projects'), pointed out that from the Parnaíba River towards the SMB, climatic conditions change from semi-arid to humid with strongest rainfall periods, tide range changes from *meso* to macro tides, the shelf becomes wider, with upwelling events and higher primary production (Class I). It represents the passage from the so characterized East Brazil shelf Large Marine Ecosystem (LME) to the North Brazil shelf LME (Knoppers et al., 1999; Ekau and Knoppers, 2003).

3. Methods

### 3.1. Oceanographic cruises and sampling

The first cruise started in October 19th 2012, collecting samples along 57 stations distributed in 12 transects perpendicular to the coast and returned in October 26th 2012. It covered an area of approximately 13.000 km², from latitude 3°S to 5°S and longitude 35.5°W to 38.5°W.

The sampling grid in Fig. 3 included the continental shelf between the isobaths of 10 to 1000 m. This area represents a narrow portion in relation to other Brazilian continental margins, inserted in a typical oligotrophic system, with tropical dry to semi-arid climatic conditions. It aimed to obtain a first screening of the area in relation to fCO_2 in the air and in the seawater, and to observe the variability between the inner and external shelves as well as the influence of rivers and continental discharges.

The second cruise, carried out from September 7th to the 14th, 2014, proposed a broader sampling grid of the Brazilian continental shelf westwards. Altogether, there were 20 sampling stations, distributed
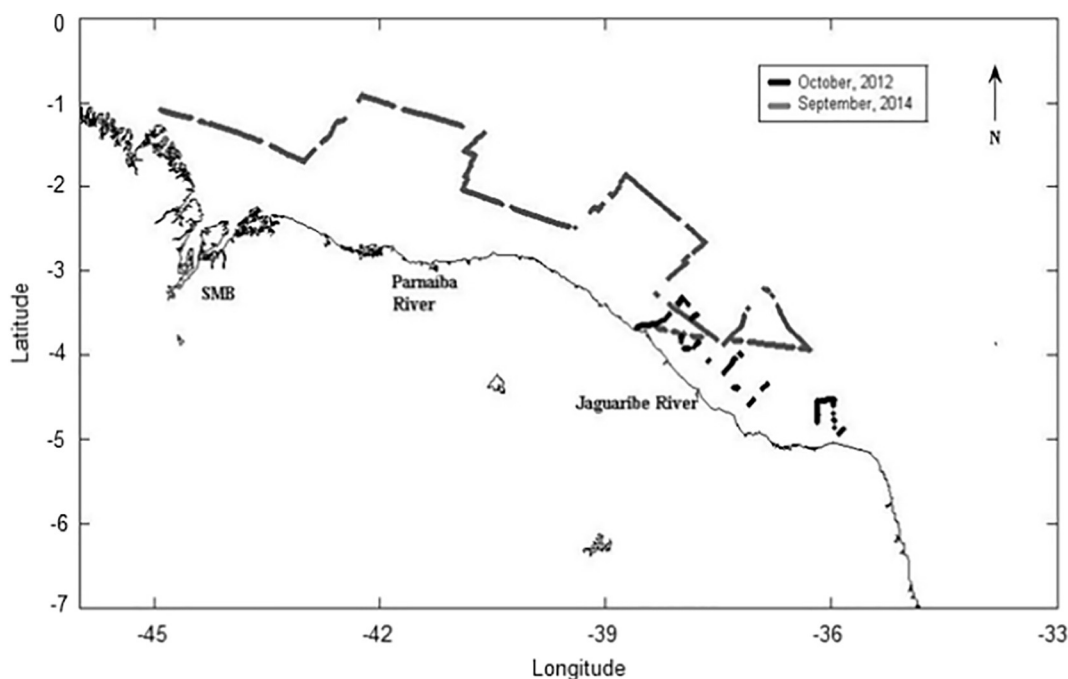
Fig. 1. Cruises' transects in the South Equatorial Atlantic Ocean adjacent to the Brazilian NE continental shelf. First cruise (October 2012) covered a smaller area. The sampling area advanced westwards in the second cruise (September 2014).
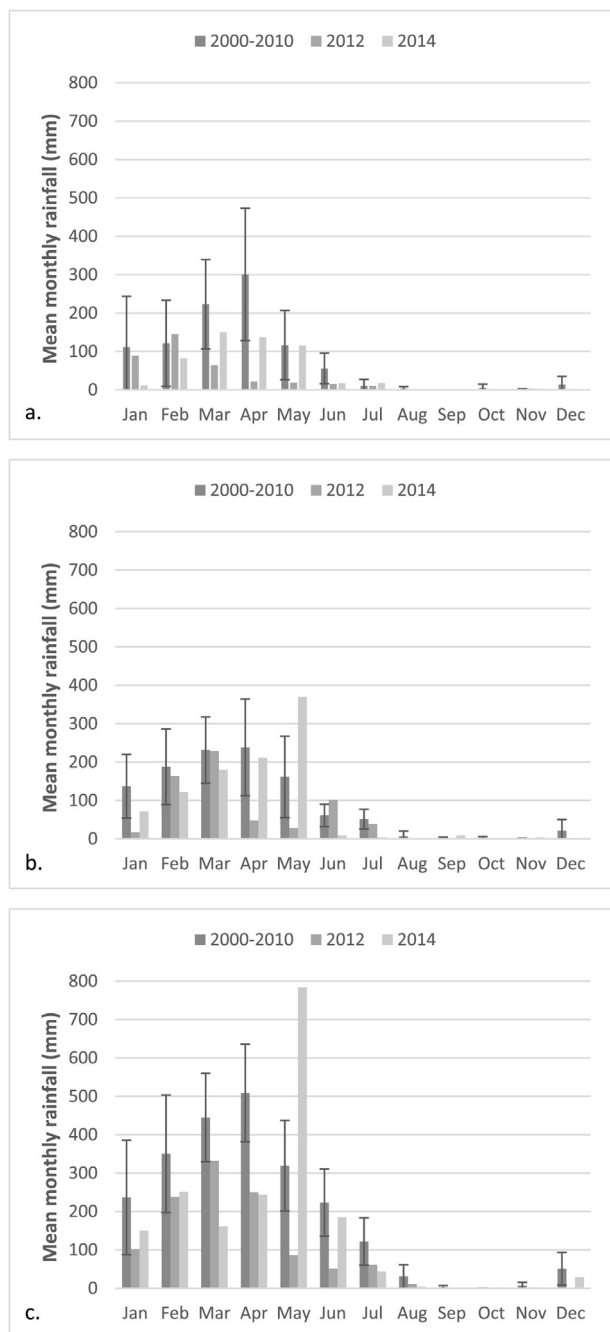
Fig. 2. Historical monthly mean (2000–2010) of rainfall for the 3 regions a. Jaguaribe, b. Parnaíba and c. SMB, compared to the years of 2012 and 2014. The bar represents the standard deviation of historical averages.

over five transects, covering an area of approximately 66.000 km² (Fig. 4). This area, extending from the Jaguaribe River to near the São Marcos Bay, represents a larger and wider portion of the Brazilian continental shelf, less oligotrophic and more humid.

A pCO_2 underway measuring system was installed on board in both cruises. The first cruise used French equipment, assigned for the bilateral cooperation agreement between France and Brazil. In the second cruise pCO_2 measurements were made using a Brazilian prototype, similar to the French system. Other pertinent data (i.e. sea surface temperature, sea surface salinity and wind speed) were collected continuously. Surface seawater samples were collected at each station for chlorophyll a, nutrients and dissolved organic carbon analysis.

3.2. Hydrographic and meteorological measurements

Sea surface temperature and salinity were obtained from SBE 21 SeaCAT Thermosalinograph every 10 s during both cruises. Surface salinity, in this case, was determined from conductivity salinity using the practical salinity scale (UNESCO, 1985). For the October 2012 cruise, wind speed velocity (wsp) was obtained through the ECMWF portal (European Centre for Medium-Range Weather Forecasts) (http://data-portal.ecmwf.int/), with a spatial resolution of 1.5° latitude by 1.5° longitude. For the September 2014 cruise, wind speed data was collected directly from the meteorological station at the NHo·Cruzeiro do Sul, where wind speed was regularly registered at 30 min intervals.

3.3. Chlorophyll a, nutrients and dissolved organic carbon (DOC)

The chlorophyll a (Chl a) analysis followed the method for determination of Chl a in seawater (Jeffrey and Humphrey, 1975). At each sampling station, surface water (5 L) was collected, filtered and refrigerated on board. The extraction of Chl a was made at the laboratory followed by spectrophotometry analysis (Micronal AJX-6100-PC model).

Absorbance measurements for phosphate and silicate were made using a spectrophotometer (Genesys 2 – Bausch & Lomb) with wavelengths of 880 nm for phosphate and 810 nm for silicate. The precision of the method is ± 0.01 μM for phosphate and ± 0.02 μM, for silicate (Grasshoff et al., 1999).

Only for the September 2014 cruise, additional analysis of dissolved organic carbon (DOC) was performed using a HyperTOC Analyzer (THERMOScientific) programed with the UV-persulphate (UV_NPOC) oxidation method (THERMO, 2008).

3.4. fCO₂ surface seawater and atmosphere measurements.

Both pCO_2 underway measuring systems used in the cruises work as described by Pierrot et al. (2009), using air-water equilibrators and an infrared analyzer for CO_2 quantification. A continuous flux of surface seawater (approximately 2.5 L min⁻¹) supplied by the vessel's pump equilibrates with air taken from the top of the vessel (at 10 m high to avoid any contamination from the ship smoke). The gas, free from humidity, passes through a non-dispersive infrared analyzer (LI-COR®, model LI-7000 CO_2/H_2O gas analyzer) for measurements of CO_2 concentrations in the seawater and in the atmosphere.

An electronic device using a LabVIEW 7.0 software controls the pCO_2 system. The program recorded and averaged the following parameters every 5 min: date and time, position of the ship, velocity of the ship, molar fraction of CO_2 in the equilibrator (xCO_2^{eq}), water content in the detector, sea surface temperature (SST) and sea surface salinity (SSS). After every 6 h of seawater molar fraction recording, atmospheric measurements were taken followed by a cycle of standards: air free from CO_2 (N_2 standard) followed by CO_2 standard gases with concentrations of 286.4 ppm, 359.8 ppm and 506.6 ppm (99.9% purity, supplied by White Martins Gases Industriais Ltda.), which were circulated through the system for comparative measurements.

The partial pressure of CO_2 in the equilibrator was computed from the molar fraction of CO_2 in dry air (xCO_2 expressed in ppm) using:

$$pCO_2^{eq} = xCO_2^{eq} (Peq - Pw(eq)) \tag{1}$$

Peq is the barometric pressure at equilibration (assumed to be the same as the atmospheric pressure at the sea surface) and Pw(eq) is the water vapor pressure (in atm) calculated at the equilibrator temperature from Weiss and Price (1980). The fugacity of CO_2 (in μatm) was calculated as follows (DOE, 1994):

$$fCO_2^{eq} = pCO_2^{eq} \times \exp[(B + 2\delta)Patm/RT] \tag{2}$$

where $B = -1636.75 + (12.0408\ T) - (0.0327957T^2) +$
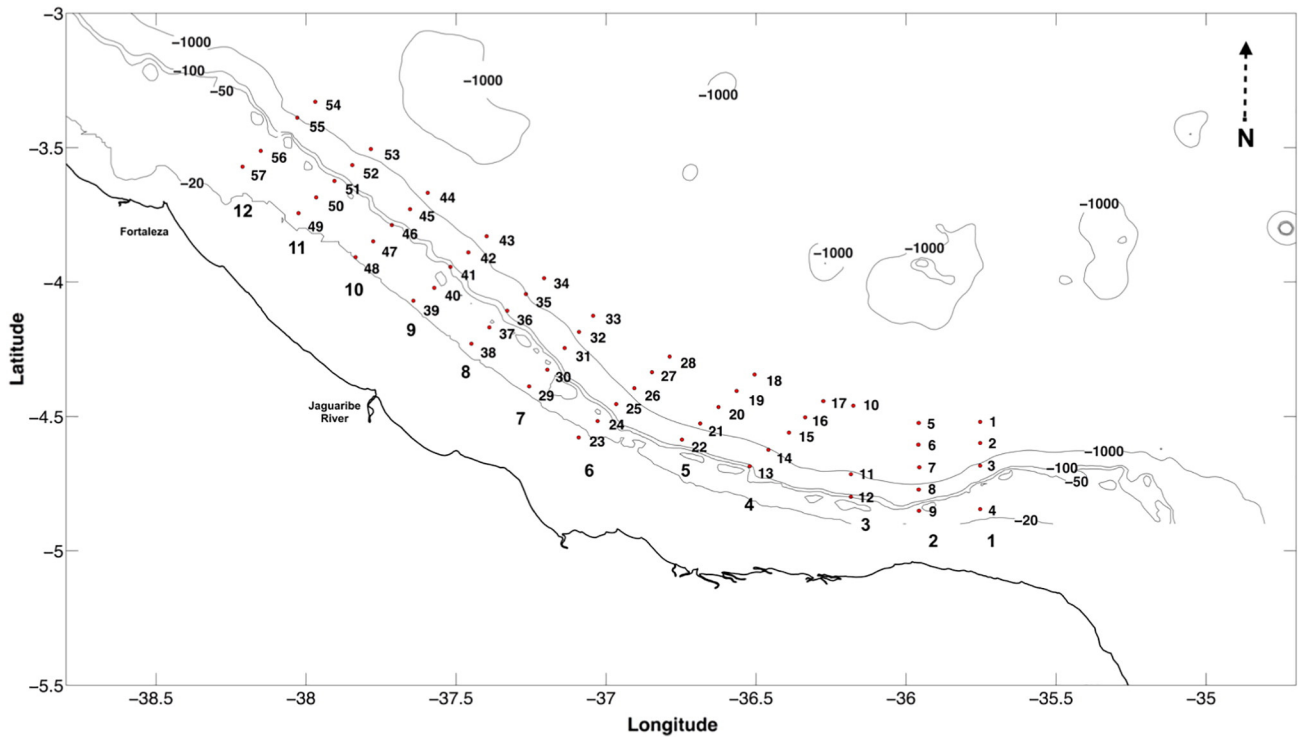
Fig. 3. Location of sampling stations in the first campaign (October 2012). A dense sampling grid with 12 transects off the continental shelf eastwards Fortaleza covering 57 stations.

(0.0000316528 T^3), T is the equilibrator temperature in Kelvin, δ = 57.7–0.118 T and $R = 8.31$ J K^{-1} mol^{-1}. A temperature correction, using the formula given by Takahashi et al. (1993), was made to convert the fugacity of CO_2 (in µatm) in the equilibrator to the fugacity of CO_2 at

the sea surface temperature (fCO_2^{sw}):

$$fCO_2^{sw} = fCO_2^{eq} \times \exp[0.0423 \times (SST-Teq)] \qquad (3)$$
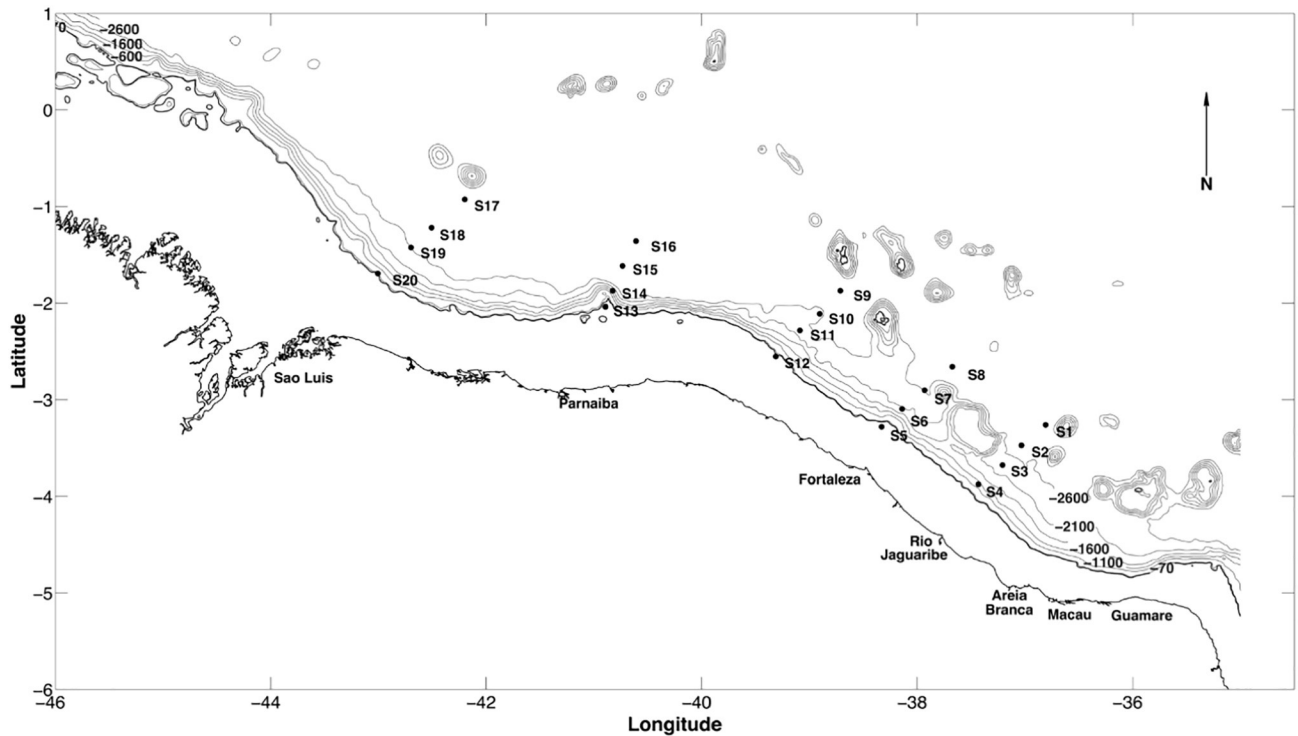
Fig. 4. Location of sampling stations in the second campaign, in September 2014. A less dense sampling grid with 5 transects off the continental shelf westwards Fortaleza covering 20 sampling stations.

For ambient air, assuming 100% vapor water saturation, the fugacity of CO_2 in the atmosphere (fCO_2^{air}) was calculated from the molar fraction of atmospheric CO_2 (xCO_2^{air}):

$$fCO_2^{air} = xCO_2^{air} \times (Patm - Pw(SST)) \times \exp[(B + 2\delta)Patm/RT] \qquad (4)$$

Patm is the atmospheric pressure and Pw(SST) is the water vapor pressure at the sea surface. The accuracy of the fugacity of CO_2 in seawater and in air is estimated at ± 2 μatm.

3.5. Calculation of CO_2 air-sea flux

The net sea-air CO_2 fluxes (F, mmol m^{-2} d^{-1}) were then calculated using:

$$F = k\,K_0\,(fCO_{2sw} - fCO_{2air}) \qquad (5)$$

where K_0 is the solubility of CO_2 as a function of SST and SSS (Weiss, 1974) and k is the gas transfer velocity coefficient which was determined previously by many authors (Wanninkhof, 1992; Nightingale et al., 2000; Sweeney et al., 2007; Takahashi et al., 2009). In this study, k was estimated using the recently updated formula in Wanninkhof (2014), which is consistent with wind speed product used. Sc represents the Schmidt number. A positive flux means a source of CO_2 to the atmosphere.

$$k = 0.251\,U_{10}^2\,(Sc/660)^{-0.5} \qquad (6)$$

3.6. Data processing and statistical analysis

SST, SSS and fCO_2 data measured continuously were processed using MATLAB® routines. To obtain the horizontal distribution of state parameters (SST, SSS and fCO_2), a grid over the entire sampled area was constructed to facilitate the visualization of the spatial distribution of the surface. The characteristic area of influence of each sample was determined using Voronoi polygons (Aurenhammer and Klein, 1996).

The vertical scale was 1.0 m, which is the resolution of the reduced data and the representative area given by Voronoi polygons. It consists of the positioning of a convex polygon plan in which each polygon contains exactly the genitor sampling station and all the area closer to the sampling point values from its next adjacent station (Okabe et al., 2008; Aurenhammer and Klein, 1996). Along the external perimeter when the use of polygons was not possible, the 20 and 70 m isobaths or the intersections between the stations alignments were used. The data were interpolated and subjected to quality control. To detect and eliminate spurious data, a Gaussian filter based on the gradient of each property was adopted, establishing a maximum range of variation for each property and eliminating any value that exceeded that range (eliminated any values larger or smaller than three times the standard deviation of each range). The uncertainty level is <5%.

Although fCO_2, SST and SSS data were obtained continuously, parameters such as Chl a and nutrients were collected punctually at each station in both cruises. To investigate the relation between these parameters (fCO_2, SST, SSS, wsp, Chl a, SiO_2^- and PO_4^{3-} and DOC for the second cruise) and fCO_2 spatial distribution, we performed statistical tests and analysis. For the first cruise, only in 27 stations all parameters were in good quality for statistical analysis and, in the second cruise, 15 stations data were used for statistical analysis. As n < 30 for each cruise, data normality was verified by Shapiro-Wilk test. As data presented non-parametric distribution, we used the Spearman's rank correlation coefficient to check correlation between them. After data normalization by z scores, we used cluster analysis to classify stations by groups according to the similarities of their parameters using Ward's method by square Euclidian distances.

3.7. $\delta^{13}C$ measures

The carbon isotopic composition of the dissolved organic matter pre concentrated using the Dittmar et al. (2012) procedures was determined, during the second cruise, using an elemental analyzer Flash 2000, with an interface Conflo IV, combined to the mass spectrometer Delta V Advantage (Thermo Scientific IRMS). The analytical control was performed by sampling reproductions (triplicates <10%) and certified standards (Elemental Microanalysis Protein Standard) above 95% of precision (Rezende et al., 2010).

4. Results

4.1. Physical and biological settings

In the first cruise, wsp ranged from 7.3 to 9.1 m s^{-1} and in the second cruise, from 5.7 to 14.9 m s^{-1}. Wind data variation found in the second cruise shows the difference between data collected in situ, with local and temporary wind effects, and data from wind fields from ECMWF, which represent daily means with smoother variations as obtained for the first cruise. Andrié et al. (1986), during the FOCAL cruises, found wsp velocities varying from 4.45 to 6.20 m s^{-1} between 0°–5°S in 35°W also using data from ECMWF reanalysis data sets.

For both cruises, sea surface temperature (SST) and sea surface salinity (SSS) values presented small variations. The mean SST for the first cruise was 26.73 ± 0.14 °C and mean SSS was 36.45 ± 0.24. In the second cruise, in September 2014, the mean SST was 26.8 ± 0.2 °C and mean SSS was 36.1 ± 0.2. For October 2012, SST and SSS presented regions with SST > 27 °C and SSS > 37 near the coast between 36.5°W and 37°W and in regions further away from the coast. We also observed higher salinities near the Jaguaribe River, where salinities are usually higher than the adjacent continental shelf (S > 39) due to high evaporation rates in relation to rainfall and to river damming (Marins et al., 2003). For September 2014, SST distribution was very homogeneous whereas SSS, west of 40°W with values higher than 36 were found. Further east the 40°W there is a big red area stressing SSS values higher than 36 intermixed with lower salinities (SSS < 35.5). Measurements in the tropical Atlantic (5°S–0°) in 1995 found mean SST varying from 28.2 ± 0.2 °C in April to 26.2 ± 0.1 °C in October (Lefèvre et al., 1998). During the dry season, the input of freshwater from the continent is negligible, without significant precipitation events and high evaporation rates resulting in small variations over SST and SSS.

Fig. 5 shows the distribution of SST and SSS data on a TS diagram and reveals, for October 2012, the presence of Tropical Water (TW), whose thermohaline indexes indicate water with temperatures higher than 26 °C and salinities higher than 36.2. However, with increasing ratio between the vertical and horizontal scales, at the stations near the coast, a gradual increase in temperature is observed ($T > 27$ °C) and salinities exceed 36.5, with almost verticality of isopycnals. For September 2014, SST and SSS spatial distribution also shows the presence of TW ($T > 26°$ C and $35 < S < 36.5$) and data homogeneity by small slope of isopycnals.

In the cruise held in October 2012, forty percent (40%) of the hydrographic stations were located within the continental shelf (depth < 70 m) increasing the aspect ratio of the physical processes (ratio between the horizontal and vertical processes). The decrease in depth associated small rainfall and high evapotranspiration process, semi-arid climate characteristics, increase of the density of tropical water mass (TW) on the continental shelf, whose TS indices are above the isopycnal 24 ($\sigma_t > 24$) (Fig. 5a). This behaviour is corroborated in the Fig. 5b, where 98% (98%) of the hydrographic stations are outside of the continental shelf (depth > 70 m), resulting in TS indices below 24 isopycnal ($\sigma_t < 24$).

Chlorophyll a (Chl a) concentration in the surface was low during both cruises. The mean Chl a values were 0.09 ± 0.09 μg L^{-1} during October 2012, and 0.12 ± 0.08 μg L^{-1} during the September 2014 cruise. The results obtained during the oceanographic expeditions of REVIZEE
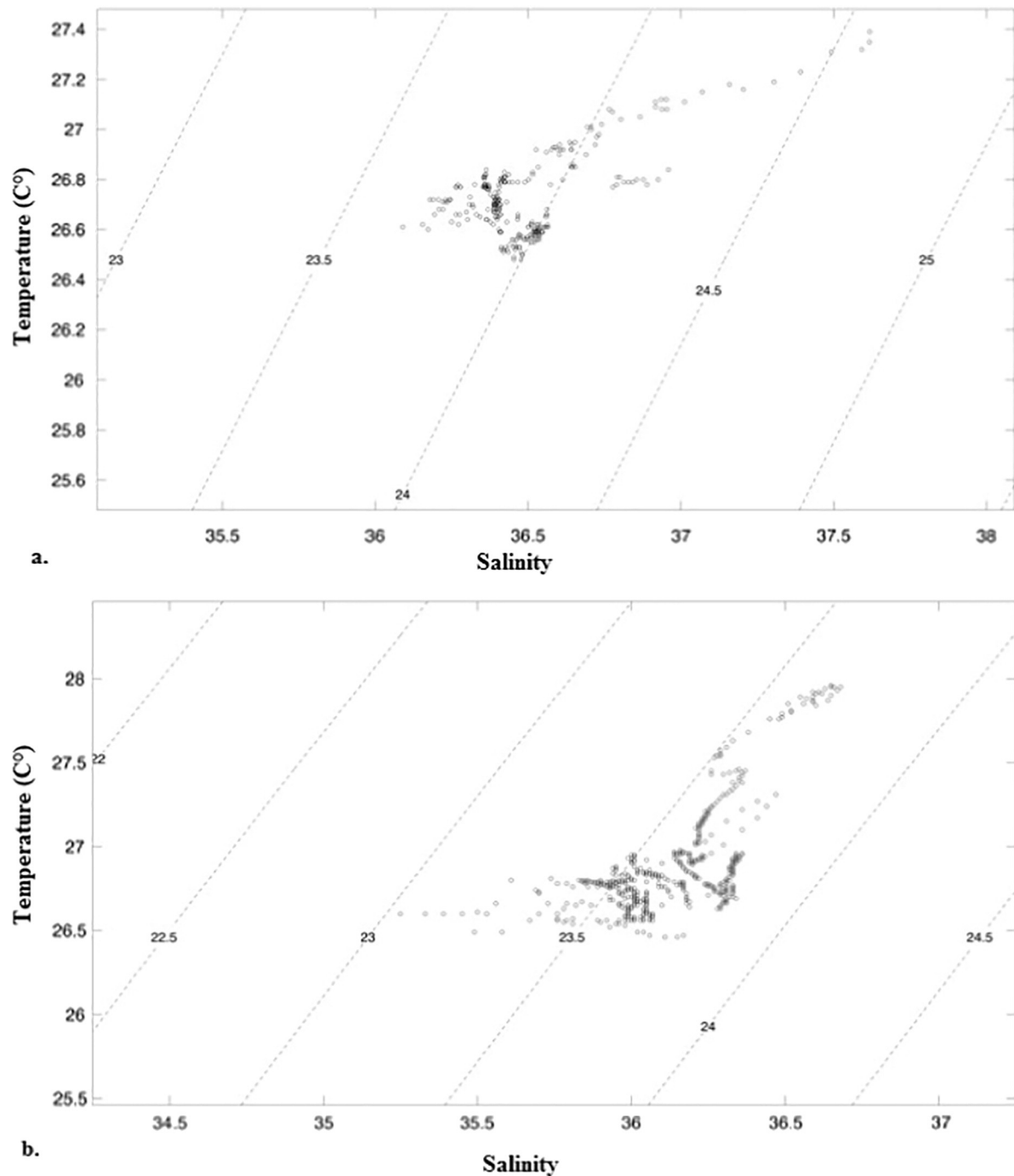
Fig. 5. Diagram showing the relationship between sea surface temperature and salinity during a) October 2012 and b) September 2014.

Table 1
Mean values (± standard deviation), minimum, maximum and number of measurements (n) of the chlorophyll *a* and nutrients at the stations during each cruise.

Cruise	Chl *a* (µg L^{-1})	Si-SiO$_2^-$ (µmol L^{-1})	P-PO$_4^{3-}$ (µmol L^{-1})	DOC (µM)
Oct 2012	(n = 58)	(n = 58)	(n = 58)	(n = 18)
Mean	0.09 ± 0.09	2.53 ± 2.57	0.17 ± 020	53.7 ± 8.2
Min	0.01	0.07	0.03	40
Max	0.63	11.28	0.92	67.5
Sep 2014	(n = 20)	(n = 20)	(n = 20)	(n = 18)
Mean	0.12 ± 0.08	3.72.9 ± 2.36	0.21 ± 0.34	53.7 ± 8.2
Min	0.02	0.52	0.02	40
Max	0.40	9.68	1.15	67.5

program for the Brazilian northeast ranged from 0.01 and 2.84 µg L^{-1} during the dry season (Mafalda et al., 2009).

For both cruises, in general, nutrient concentrations were low. Silicate showed the highest concentrations with a mean of 3.72 ± 2.36 µmol L^{-1} in the first cruise and 2.92 ± 2.54 µmol L^{-1} in the second cruise. Phosphate values were also low with mean values of 0.19 ± 0.20 µmolL^{-1} for the first cruise and 0.21 ± 0.34 µmolL^{-1} for the second cruise (Table 1).

For September 2014, DOC concentrations ranged between 40 and 67.5 µM, with mean concentration of 53.7 µM. The transect adjacent to the SMB region had the highest mean DOC value of 62.1 µM. Mean DOC concentrations found in the continental shelf adjacent to the Parnaíba and Jaguaribe River were 58.5 µM and 48.3 µM, respectively.

DOC levels measured in the Brazilian Northeast continental shelf were lower than the expected for tropical systems (70–80 µmol kg^{-1}) (Hansell et al., 2009). High fresh water inputs into some regions of the tropical ocean due to the presence of large rivers like the Amazon, Orinoco and others (Dai et al., 2012) imply in high DOC concentrations, whereas low river inputs to the continental shelf during the dry season (Dias et al., 2013) in the study site leads to low DOC concentrations.

There are no previous measurements of DOC in this region of the Brazilian northeast continental shelf, mean DOC concentrations in the continental shelf adjacent to the SMB and the Parnaíba River were similar to those observed in oligotrophic waters from the Mediterranean Sea, which ranged between 57 and 68 µM (Santinelli et al., 2010). Low concentrations of DOC (56–76 µM) were also recorded in coastal waters of the northern Tyrrhenian Sea during a period of weak flow caused by meteorological conditions (Vignudelli et al., 2004).

However, DOC levels near the Jaguaribe River were even lower, like those estimated by remote sensing in the middle continental shelf of the China Sea (~45 to 60 µM). These low values correspond to the oligotrophic zone of the China Sea caused by upwelling events that brings DOC-poor waters to surface (Pan et al., 2013, Pan and Wong, 2015).

4.2. Distribution of fCO₂ in the surface seawater and the atmosphere

In October 2012, the mean of fCO_2^{sw} was 400.2 ± 6.0 µatm and fCO_2^{air} was 375.8 ± 2.0 µatm. The lower value of fCO_2^{sw} was 388.3 µatm in the regions east of the Jaguaribe River and the highest value reached 413.9 µatm near Fortaleza, in regions west of the Jaguaribe River. In the second cruise, in September 2014, fCO_2^{sw} values ranged from 371.9 µatm to 411.7 µatm and the mean value was 391.2 ± 6.4 µatm. The highest values were found near the SMB. The mean fCO_2^{air} value was 368.9 ± 2.2 µatm, the maximum fCO_2^{air} value found was 371.9 µatm and the minimum fCO_2^{air} was 363.6 µatm (Table 2). These fCO_2^{air} values are in the same range of recently reported values for the west equatorial Atlantic Ocean (Ibánhez et al., 2016; Lefèvre et al., 2014). The fCO_2^{air} values of the entire surveyed area were lower than the fCO_2^{sw} but still very close, with ΔfCO_2 ranging from +12.5 to +61.6 µatm in the first cruise and from +4.1 to +48.2 µatm in the second cruise. The fCO_2^{sw} distributions for the different sampling periods are shown in Fig. 6.

4.3. Statistics

A Spearman correlation matrix of fCO_2 distribution along the study area with seawater properties such as SST, SSS, *wsp*, nutrients and Chl *a* for the first cruise is presented in Table 3a. DOC was included for the cruise of September 2014 in Table 3b.

For October 2012, the only significant correlation found was between fCO_2^{sw} and SSS while the other variables showed no significant correlation with fCO_2^{sw}, corroborating with Dias et al. (2013) observations of oceanic intrusion. In this portion of the continental shelf, during this season, we can infer that the SSS is the parameter that most influences the variability of the fCO_2^{sw} and that this region has a similar behaviour to the open ocean waters, probably being controlled by physical parameters throughout the year.

However, for the September 2014, with broadening of the study area, reaching receptors of larger rivers in the westernmost part of the continental shelf than the area covered in 2012, it was found significant positive correlations between fCO_2^{sw} and physical parameters such as: SST, SSS, *wsp* but also with Chl *a* and silicate (Si-SiO$_2^-$) and a negative correlation with phosphate (P-PO$_4^{3-}$) appears (Table 3b).

This suggests that, despite the low values measured for both Chl *a* and nutrients, they seem to influence the CO_2 processes in a larger portion of the coast. Probably showing differences between ocean and continental influences from the eastern to the western equatorial coast, with the predominance of ocean forcing at the east.

Phosphorus is absorbed by phytoplankton in the sea surface and together with Nitrogen are limiting nutrients for the photosynthetic activity (Downing, 1997). With the increase of Chl *a*, a decrease in fCO_2 was expected. There was no significant correlation between fCO_2 and DOC.

The cluster analysis revealed two distinct groups A and B (Fig. 7). Group A containing only October 2012 stations (Stations starting with 'O' are related to the first cruise) and Group B containing September 2014 stations (Stations starting with 'S' are for stations of the second cruise) and stations of the first cruise (O23 O24 O26 O27) which belong to the same transect (transect 6). It was observed that the subgroups formed separated stations located in the eastern regions from stations in western regions. In general, the stations of the same transect belonged to the same group, showing homogeneity along the transect and the heterogeneity observed was longitudinal, between east and west, reinforcing the hypothesis of transition between two different behaviour areas as we moved to the west.

For October 2012, it was observed no variation between the inner and external continental shelf, showing that during the dry season, the continental influence was not enough to be found off in the ocean. The longitudinal variations (west to east) are more evident. For September 2014, stations of transects 1 and 2 were grouped in subgroup B1 together with October stations from transect 6, and transects 3, 4, 5 and formed a subgroup B2. This separation is probably marking the transition between distinct behaviour areas, as it was observed that highest fCO_2 values were found in stations 3, 4 and 5 compared with lowest fCO_2 values of transects 1 and 2.

In addition to the relationships between CO_2 and physical and chemical parameters, the influence of the continental contribution can be observed by the $\delta^{13}C$ distribution in the dissolved organic matter, along the study area where lighter $\delta^{13}C$ values predominated in the portions of the continental shelf under stronger influence of river discharges (Fig. 8) (Mangrove: $\delta^{13}C$ −27.9 ± 1.4‰ and Phytoplankton: $\delta^{13}C$ −21.0 ± 0.8‰) (Fry et al., 1998; Kuramoto and Minagawa, 2001; Rezende et al., 2010). Also of notice is the existence of the world largest continuous mangrove forest bordering the western portion of the studied area. This forest is a significant carbon source to the continental shelf in the region (Lacerda et al., 2001).

4.4. Air-sea CO₂ flux in the Brazilian equatorial northeast coast

The air-sea flux obtained by calculation was positive for both cruises, indicating that the region works as a source of CO_2 for the measured periods, as a consequence of the tropical Atlantic high fCO_2 values.

The average CO_2 fluxes for the first cruise period was +3.28 ± 1.07 mmol m^{-2} d^{-1}. The maximum flux value reached +7.24 mmol m^{-2} d^{-1} and occurred in the transect nearby Fortaleza. The lowest flux value was +1.66 mmol m^{-2} d^{-1}.

The estimated flux for September 2014 was also positive throughout the course of the cruise and the mean value was 5.87 ± 3.06 mmol m^{-2} d^{-1}. The flux values reached a maximum of 14.62 mmol m^{-2} d^{-1} in 41°W and a minimum value of 0.89 mmol m^{-2} d^{-1} in 37°W.

Table 2
Mean values (± standard deviation), minimum, maximum and number of measurements (n) of the fugacity of CO_2 in surface water (fCO_2^{sw}) and in the atmosphere (fCO_2^{air}), SST, SSS and wind speed for each cruise.

Cruise	fCO_2^{sw} (µatm)	fCO_2^{air} (µatm)	SST (°C)	SSS (psu)	wsp (m.s^{-1})
Oct 2012	(n = 310)	(n = 14)	(n = 433)	(n = 433)	(n = 415)
Mean	400.9 ± 7.31	375.8 ± 2.0	26.73 ± 0.14	36.45 ± 0.24	8.1 ± 0.52
Min	388.3	373.1	26.48	36.09	7.3
Max	428.7	378.6	27.39	37.6	9.1
Sep 2014	(n = 1069)	(n = 1069)	(n = 1069)	(n = 1069)	(n = 1104)
Mean	391.1 ± 6.3	368.9 ± 2.2	26.8 ± 0.2	36.1 ± 0.2	11.2 ± 2.07
Min	371.9	363.5	26.5	34.3	5.7
Max	411.7	371.9	28	36.7	14.9

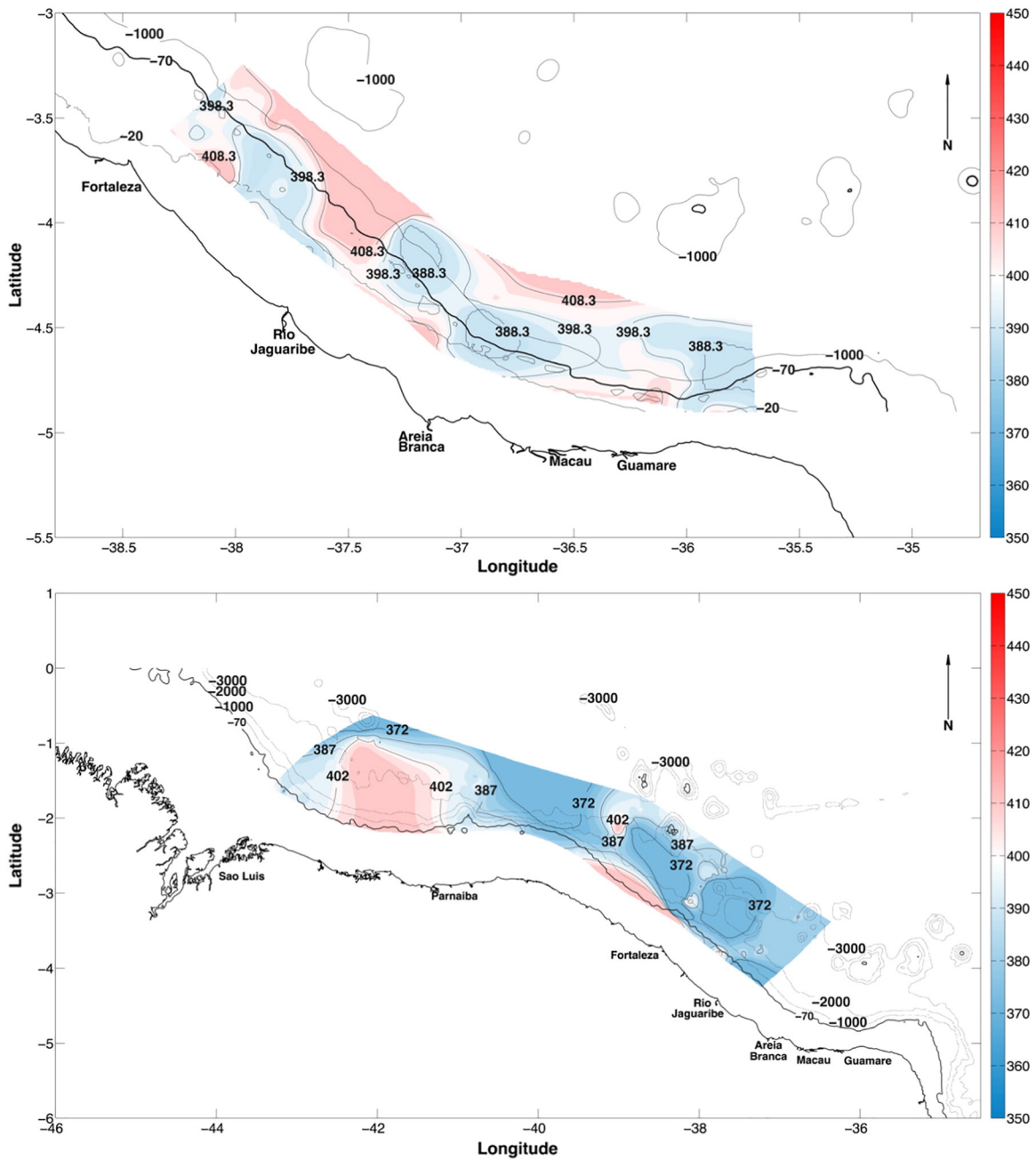**Fig. 6.** a) fCO_2^{sw} spatial distribution during the first campaign, October 2012. b) fCO_2^{sw} distribution during the September 2014 campaign.

Andrié et al. (1986) found global mean net CO_2 flux from the ocean to the atmosphere of 1.05 mmol m^{-2}d^{-1} between 5°N and 5°S. They also found that the release of CO_2 increases from east to west. Lefèvre et al. (2014) calculated the mean CO_2 fluxes for March 2009 and July 2010 and found the area south of 2.5°S as a strong source of CO_2 with fluxes >3 mmol m^{-2} d^{-1}.

Plotting the CO_2 flux values of the two cruises together, the values obtained for the first cruise are in the same range as those obtained in

Table 3a
Spearman's rank correlation coefficients for variables of the October 2012 cruise (n = 27).

	fCO_2^{sw}	SST	SSS	Wsp	Chl a	Si-SiO$_2^-$	P-PO$_4^{3-}$
fCO_2^{sw}	1						
SST	0.26	1					
SSS	−0.62*	−0.40*	1				
Wsp	0.32	0.29	−0.46	1			
Chl a	−0.24	−0.19	0.24	−0.32	1		
Si	0.26	0.21	−0.05	−0.02	0.01	1	
P-PO$_4^{3-}$	0.10	0.20	−0.23	0.34	−0.16	0.37	1

* Marked correlations are significant at p < 0.05.

Table 3b
Spearman's rank correlation coefficients for variables of the cruise of September 2014 (n = 15).

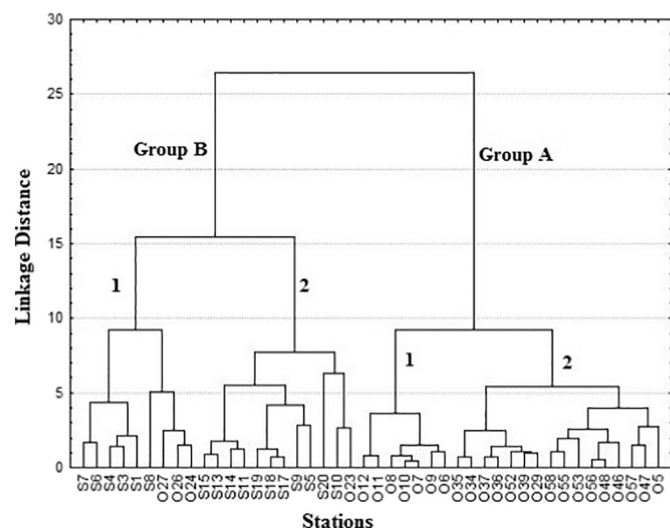|	fCO_2^{sw}	SST	SSS	Wsp	Chl a	Si-SiO$_2^-$	P-PO$_4^{3-}$	DOC
fCO_2^{sw}	1							
SST	0.56*	1						
SSS	0.53*	0.15	1					
Wsp	0.61*	0.16	0.74*	1				
Chl a	0.51*	0.16	0.58*	0.60*	1			
Si	0.52*	0.24	0.28	0.37	0.28	1		
P-PO$_4^{3-}$	−0.75*	−0.63*	−0.41	−0.60*	−0.40	−0.35	1	
DOC	0.39	0.52*	0.56*	0.41	0.53*	−0.04	−0.70*	1

* Marked correlations are significant at p < 0.05.

Fig. 7. Cluster Analysis of fCO_2 and physical and chemical parameters measured in the studied area. Stations starting with 'O' October 2012 cruise; Stations starting with 'S' are from September 2014 cruise.

the same longitudes during the second cruise (Fig. 9), showing good agreement between data in the same region and in the same season.

Studies assessing the variations of this source over time have led to different conclusions (Andrié et al., 1986; Oudot et al., 1995), there is no consensus over this subject yet. Local increase or decrease of fCO_2 can be induced by vortices and may be associated with current circulation. More data need to be evaluated to better detect CO_2 trends in the Tropical Atlantic (Lefèvre et al., 2014).

5. Discussion

This study presents fCO_2^{sw}, fCO_2^{air} and CO_2 fluxes for an under sampled region of the Brazilian Northeast continental shelf. Despite the small variability expected for this region, a transition of behaviour was

revealed between east and west. This highlights the importance of coastal zones measurements as they can present such a different behaviour when compared to global ocean areas.

For the cruise of October 2012, a condition of limited continental influence, during the sampled period, with the predominance of the intrusion of oceanic water in the continental shelf seems to be dominant during that cruise. The origin of CO_2 in this region, in the dry season, probably comes from tropical oceanic waters super-saturated with CO_2 instead of continental contributions. A strong oligotrophic condition is predominant and the primary production is very low in this region during this time of the year. The influence of the terrestrial fluxes of organic matter to the oceans through rivers, observed in many regions of the world (Ludwig et al., 1996), do not occurred here where the rivers' influence depends on an expressive rainy season that does not always occur.

Dias et al. (2013), during an extreme period of maximum river discharge of the Jaguaribe River measured a 6 km long estuarine plume, whose influence extends only to the inner continental shelf and restricted to a 2 meters depth layer at the surface. This indicates that the intrusion of tropical water on the continental shelf is stronger than the continental influence, even when it does exist.

However, in October 2012, the fCO_2^{sw} showed minimum values near the Jaguaribe River contribution. This suggests that only during a strong rainy season, this river may transport nutrients enough to enhance primary production and change the CO_2 behaviour locally.

In September 2014, the minimum values of fCO_2^{sw} occurred also in the continental shelf adjacent to the Jaguaribe and Parnaíba River contributions. This leads to the hypothesis that after severe rainy season, stronger river discharges with more nutrients reaching the coast together with good light penetration, primary production would be enhanced and CO_2 could be absorbed. The fCO_2^{sw} values increased westwards showing maximum values adjacent to the São Marcos Bay. At the SMB, high turbidity and action of macrotides (>6 m) are the main causes of the small thickness of the photic zone due to rapid attenuation of light energy, thus causing reduction in absorption of light by phytoplankton and thus reducing photosynthesis (Azevedo et al., 2008). These characteristics combined with higher SSS (>36) measured during the cruise near the influence of SMB may favor the increase of fCO_2.

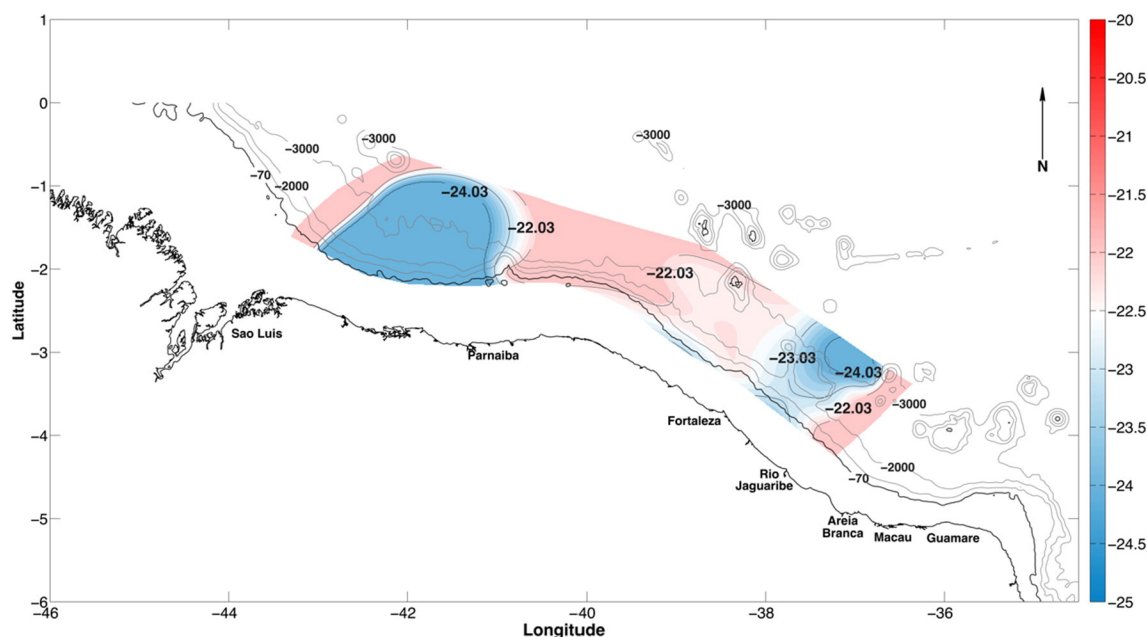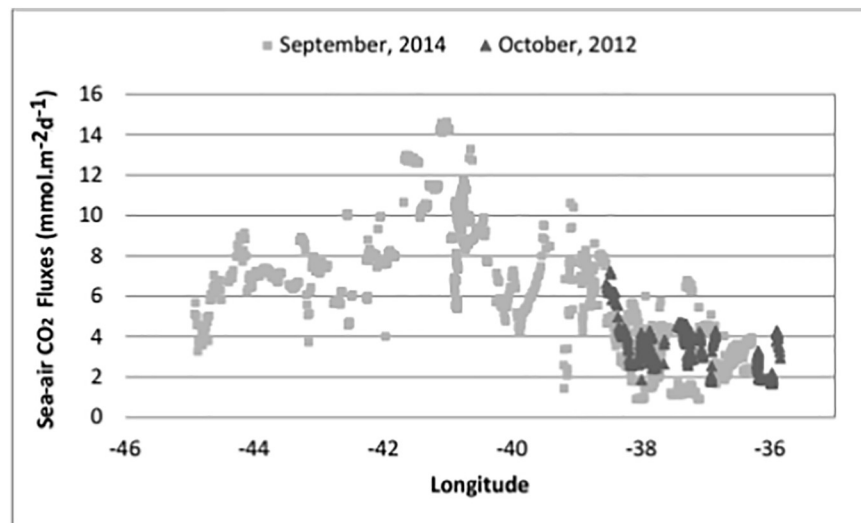**Fig. 8.** $\delta^{13}C$ distribution in the dissolved organic matter sampled during the September 2014 cruise.

Fig. 9. Sea-air CO_2 fluxes calculated for the two cruises at the Brazilian Northeastern shelf.

5.1. fCO₂ measurements in the tropical Atlantic

High fCO_2^{sw} values were measured in other studies in the Tropical Atlantic usually characterizing it as a source of CO_2 to the atmosphere (Andrié et al., 1986; Goyet et al., 1998; Lefèvre et al., 2013). FOCAL Cruises 2, 4, 6 and 8 between 0 and 5°S along 35°W found pCO_2^{sw} between 365 and 408 µatm. Goyet et al. (1998) measurements in the Tropical Atlantic Ocean between 7°30′N and 32°S along 19°W during WOCE A15 found pCO_2^{sw} results resembling those found during FOCAL cruises but an increase of 10 µatm in pCO_2^{air}, indicating a decrease on CO_2 supply to the atmosphere. Further measurements made in the Tropical Atlantic (20°N–20°S) attributed the supersaturation to the CO_2 supplied from equatorial and coastal upwelling (Lefèvre et al., 1998).

Surface seawater CO_2 concentrations below atmospheric levels due to the influence exerted by the Amazon River discharge, close to the 55° W, were verified by Körtzinger (2003), Lefèvre et al. (2010) and Ternon et al. (2000), but the region sampled in our cruise is not close enough to receive such influence. However, a decrease in ΔfCO_2 was evidenced in the second cruise, which reached a transition area where climatic conditions starts to change to humid in comparison with the first one where semi-arid climate domains.

5.2. Factors controlling seawater CO₂ fugacity

Temperature increase tends to enhance fCO_2, whereas biological activity is also an important factor on fCO_2 control, mainly over the coast. Based in the statistical analysis, SST was the most significantly driver of fCO_2^{sw} variation. We believe that with more frequent measurements in the region over an annual cycle, it will be possible to improve the SST-fCO_2^{sw} relation for the construction of a strong regional algorithm allowing future fCO_2^{sw} predictions to be applied to this part of the Brazilian coast.

6. Conclusion

This study represents the first screening of the distribution of the fCO_2 in the surface waters of the continental shelf off the Brazilian Equatorial Northeastern coast. Data on fCO_2^{sw} indicate that the area is supersaturated with respect to the overlying marine air causing a net CO_2 release to the atmosphere.

CO_2 annual performance needs to be improved with higher sampling frequency along the years so that we can better understand the CO_2 seasonal variations. Different characterization of the eastern and the western portion of the Northeast continental shelf showed different behaviours. The eastern part of the shelf works similarly to the open ocean regarding fCO_2, influenced by physical parameters, mostly SSS, whereas the western part of the shelf seems to have a more complex behaviour influenced by physical parameters such as SST, SSS and *wsp* but also by nutrients and Chlorophyll *a*. Even with small concentrations, Chl *a* and nutrients seem to have a significant importance on fCO_2^{sw} distribution on this continental margin.

Anthropogenic impacts to the coastal and estuarine waters tend to increase, with the growth of aquaculture activities and river damming in these regions, this pressure will probably affect the CO_2 behaviour. Generally, global models do not represent these areas well enough, enhancing the need for pCO_2 measurements and associated air-sea CO_2 fluxes in the continental margins. This work represents the first steps in the study of the coastal region in relation to CO_2 behaviour in this study area. In the last cruise, a Brazilian CO_2 device, constructed by an innovative technological independence effort, was used, contributing to enhance the number of field measurements of the partial pressure of CO_2 in the country's continental margins. We hope that an increase in the number of pCO_2 measurements in the continental margins can contribute to future calibration of regional and global models.

References

Andrié, C., Oudot, C., Genthon, C., Merlivat, L., 1986. CO₂ fluxes in the tropical Atlantic during FOCAL cruises. J. Geophys. Res. 91, 11741–11755.

Aurenhammer, F., Klein, R., 1996. Voronoi diagrams. Technical Report 198. Fern Universität, Hagen 92p. Available at. http://www.pi6.fernuni-hagen.de/publ/tr198.pdf.

Azevedo, A.C.G., Feitosa, F.A.N., Koening, L.M., 2008. Distribuição espacial e temporal da biomassa fitoplanctônica e variáveis ambientais no Golfão Maranhense, Brasil. Acta Bot. Bras. 22 (3), 870–877.

Bauer, J.E., Cai, W.-J., Raymond, P.A., Bianchi, T.S., Hopkinson, C.S., Regnier, P.A.G., 2013. The changing carbon cycle of the coastal ocean. Nature 504, 61–70.

Borges, A.V., Delille, B., Frankignoulle, M., 2005. Budgeting sinks and sources of CO₂ in the coastal ocean: diversity of ecosystems counts. Geophys. Res. Lett. 32, L14601. http://dx.doi.org/10.1029/2005GL023053.

Cai, W.-J., Dai, M., Wang, Y., 2006. Sea-air exchange of carbon dioxide in ocean margins: a province-based synthesis. Geophys. Res. Lett. 33, L12603.

Canadell, J.G., Le Quéré, Corinne, Raupach, Michael R., Field, Christopher B., Buitenhuis, Erik T., Ciais, Philippe, Conway, Thomas J., Gillett, Nathan P., Houghton, R.A., Marland, Gregg, 2007. Contributions to accelerating atmospheric CO₂ growth from economic activity, carbon intensity, and efficiency of natural sinks. Proc. Natl. Acad. Sci. U. S. A. 104 (47), 18866–18870.

Chen, C.-T.A., Borges, A.V., 2009. Reconciling opposing views on carbon cycling in the coastal ocean: continental shelves as sinks and near-shore ecosystems as sources of atmospheric CO₂. Deep-Sea Res. II 56, 578–590.

Chen, C.-T.A., Huang, T.-H., Chen, Y.-C., Bai, Y., He, X., Kang, T., 2013. Air–sea exchanges of CO₂ in the world's coastal seas. Biogeosciences 10, 6509–6544.

Cooley, S.R., Yager, P.L., 2006. Physical and biological contributions to the western tropical North Atlantic Ocean carbon sink formed by the Amazon River plume. J. Geophys. Res. 111. http://dx.doi.org/10.1029/2005JC002954.

Dai, M., Yin, Z., Meng, F., Liu, Q., Cai, W.J., 2012. Spatial distribution of riverine DOC inputs to the ocean: an updated global synthesis. Curr. Opin. Environ. Sustain. 4:170–178. http://dx.doi.org/10.1016/j.cosust.2012.03.003.

Dias, F.J.S., Castro, B.M., Lacerda, L.D., 2013. Continental shelf water masses off the Jaguaribe River (4S), Northeastern Brazil. Cont. Shelf Res. 66:123–135. http://dx.doi.org/10.1016/j.csr.2013.06.005.

Dittmar, T., Rezende, C.E., Manecki, M., Niggemann, J., Ovalle, A.R.C., Bernardes, M.C., 2012. Continuous flux of dissolved black carbon from a vanished tropical forest biome. Published Online: 12 August 201. Nat. Geosci. J2:618–622. http://dx.doi.org/10.1038/Ngeo1541.

DOE, 1994. In: Dickson, A.G., Goyet, C. (Eds.), Handbook of Methods for the Analysis of the Various Parameters of the Carbon Dioxide System in Seawater. ORNL/CDIAC-74.

Downing, J.A., 1997. Marine nitrogen: phosphorus stoichiometry and global N:P cycle. Biogeochemistry 37, 237–252.

Ekau, W., Knoppers, B., 2003. A review and redefinition of the large marine ecosystems of Brazil. In: Sherman, K., Hempel, G. (Eds.), Large Marine Ecosystems of the World - Trends in Exploitation, Protection and Research. Elsevier Science, Amsterdam. ISBN: 0444510273.

Fry, B., Hopkinson, C.S., Nolin, A., Wainright, S.C., 1998. ¹³C/¹²C composition of marine dissolved organic carbon. Chem. Geol. 152:113–118. http://dx.doi.org/10.1016/S0009-2541(98)00100-4.

Goyet, C., Adams, R., Eischeid, G., 1998. Observations of CO₂ system properties in the tropical Atlantic Ocean. Mar. Chem. 60, 49–61.

Grasshoff, K., Kremling, M., Ehrhardt, M., 1999. Methods of Seawater Analysis. third ed. WILEY-VCH 632p.

Gruber, N., 2015. Ocean biogeochemistry: carbon at the coastal interface. Nature 517: 148–149 http://dx.doi.org/10.1038/nature14082.

Hansell, D.A., Carlson, C.A., Repeta, D.J., Schlitzer, R., 2009. Dissolved organic matter in the ocean. Oceanography 22:202–211 http://dx.doi.org/10.5670/oceanog.2009.109.

Ibánhez, J.S.P., Araujo, M., Lefèvre, N., 2016. The overlooked tropical oceanic CO₂ sink. Geophys. Res. Lett. 43:3804–3812. http://dx.doi.org/10.1002/2016GL068020.

Ito, R.G., Schneider, B., Thomas, H., 2005. Distribution of surface fCO₂ and air–sea fluxes in the Southwestern subtropical Atlantic and adjacent continental shelf. J. Mar. Syst. 56, 227–242.

Jeffrey, S.W., Humphrey, G.F., 1975. New spectrophotometric equations for determining chlorophyll a, b c1 and c2 in higher plants, algae and natural phytoplankton. Biochem. Physiol. 167, 191–194.

Jiang, L.-Q., Cai, W.-J., Wang, Y., Bauer, J.E., 2013. Influence of terrestrial inputs on continental shelf carbon dioxide. Biogeosciences 10, 839–849.

Knoppers, B., Ekau, W., Figueiredo, A.G., 1999. The coast and shelf of east and northeast Brazil and material transport. Geo-Mar. Lett. 19, 171–178.

Körtzinger, A., 2003. A significant sink of CO₂ in the tropical Atlantic Ocean associated with the Amazon River plume. Geophys. Res. Lett. 30:2287. http://dx.doi.org/10.1029/2003gl018841.

Kuramoto, T., Minagawa, M., 2001. Stable carbon and nitrogen isotopic characterization of organic matter in a mangrove ecosystem on the Southwestern coast of Thailand. J. Oceanogr. 57:421–431. http://dx.doi.org/10.1023/A:1021232132755.

Lacerda, L.D., Conde, J.E., Kjerfve, B., Alvarez-León, R., Alarcón, C., Polanía, J., 2001. American mangroves. In: Lacerda, L.D. (Ed.), Mangrove Ecosystems: Function and Management. Springer, Berlin. ISBN: 9783642075858 http://dx.doi.org/10.1007/978-3-662-04713-2_1.

Laruelle, G.G., Dürr, H.H., Slomp, C.P., Borges, A.V., 2010. Evaluation of sinks and sources of CO₂ in global coastal ocean using a spatially-explicit typology of estuaries and continental shelves. Geophys. Res. Lett. 37, L15607.

Laruelle, G.G., Lauerwald, R., Pfeil, B., Regnier, P., 2014. Regionalized global budget of the CO₂ exchange at the air-water interface in continental shelf seas. Glob. Biogeochem. Cycles 28:1199–1214. http://dx.doi.org/10.1002/2014GB004832.

Lefèvre, N., Moore, G., Aiken, J., Watson, A., Cooper, D., Ling, R., 1998. Variability of CO₂ in the tropical Atlantic in 1995. J. Geophys. Res. 103 (C3), 5623–5634.

Lefèvre, N., Diverrès, D., Gallois, F., 2010. Origins of CO₂ undersaturation on the Atlantic. Tellus 62B, 595–607.

Lefèvre, N., Caniaux, G., Janicot, S., Gueye, A.K., 2013. Increased CO₂ outgassing in February–May 2010 in the tropical Atlantic following the 2009 Pacific El Ninõ. J. Geophys. Res. Oceans 118:1645–1657. http://dx.doi.org/10.1002/jgrc.20107.

Lefèvre, N., Urbano, D.F., Gallois, F., Diverrès, D., 2014. Impact of physical processes on the seasonal distribution of the fugacity of CO₂ in the western tropical Atlantic. J. Geophys. Res. Oceans 119. http://dx.doi.org/10.1002/2013JC009248.

Ludwig, W., Probst, J.-L., Kempe, S., 1996. Predicting the oceanic input of organic carbon by continental erosion. Glob. Biogeochem. Cycles 10, 23–41.

Mafalda Jr., P.O., Moura, G., Melo, G., Sampaio, J., Feitosa, F.A.N., Passavante, J.Z.O., Souza, M.O., Sampaio, C., 2009. Oceanografia biológica: biomassa fitoplanctônica na ZEE da Região Nordeste do Brasil. In: Fábio, V.H.H. (Ed.), Programa REVIZEE - Score Nordeste. Martins & Cordeiro, Fortaleza, pp. 11–23.

Marins, R.V., Lacerda, L.D., Abreu, I.M., Dias, F.J.S., 2003. Efeitos da açudagem no rio Jaguaribe. Ciência Hoje 33 (197), 66–70.

Nightingale, P.D., Malin, G., Law, C.S., Watson, A.J., Liss, P.S., Liddicoat, M.I., Boutin, J., Upstill-Goddard, R.C., 2000. In situ evaluation of air-sea exchange parameterizations using novel conservative and volatile tracers. Glob. Biogeochem. Cycles 1, 373–387.

Okabe, A., Boots, B., Sugihara, K., Chiu, S.N., Kendall, D.G., 2008. Spatial Tessellations: Concepts and Applications of Voronoi Diagrams. second ed. John Wiley & Sons Ltd, London 683p.

Oudot, C., Ternon, J.F., Lecomte, J., 1995. Measurements of atmospheric and oceanic CO₂ in the tropical Atlantic: ten years after the 1982–1984 FOCAL cruises. Tellus Ser. B 47, 70–85.

Pan, X., Wong, G.T.F., 2015. An improved algorithm for remotely sensing marine dissolved organic carbon: climatology in the northern South China Sea shelf-sea and adjacent waters. Deep-Sea Res. II Top. Stud. Oceanogr. 117:131–142. http://dx.doi.org/10.1016/j.dsr2.2015.02.025.

Pan, X., Wong, G.T.F., Ho, T., Shiah, F., Liu, H., 2013. Remote sensing of picophytoplankton distribution in the northern South China Sea. Remote Sens. Environ. 128:162–175. http://dx.doi.org/10.1016/j.rse.2012.10.014.

Pierrot, D., Neill, C., Sullivan, K., Castle, R., Wanninkhof, R., Lüger, H., Johannessen, T., Olsen, A., Feely, R.A., Cosca, C.E., 2009. Recommendations for autonomous underway pCO₂ measuring systems and data-reduction routines. Deep-Sea Res. II 56, 512–522.

Rezende, C.E., Pfeiffer, W.C., Martinelli, L.A., Tsamakis, E., Hedges, J.I., Keil, R.G., 2010. Lignin phenols used to infer organic matter sources to Sepetiba Bay e RJ, Brazil. Estuar. Coast. Shelf Sci. 87:479–486. http://dx.doi.org/10.1016/j.ecss.2010.02.008.

Sabine, C.L., Feely, R.A., Gruber, N., Key, R.M., Lee, K., Bullister, J.L., Wanninkhof, R., Wong, C.S., Wallace, D.W.R., Tilbrook, B., Millero, F.J., Peng, T.-H., Kozyr, A., Ono, T., Rios, A.F., 2004. The oceanic sink for anthropogenic CO₂. Science 305, 367–371.

Santinelli, C., Nannicini, L., Seritti, A., 2010. DOC dynamics in the meso and bathypelagic layers of the Mediterranean Sea. Deep-Sea Res. II Top. Stud. Oceanogr. 57: 1446–1459. http://dx.doi.org/10.1016/j.dsr2.2010.02.014.

Sweeney, C., Gloor, E., Jacobson, A.R., Key, R.M., McKinley, G., Sarmiento, J.L., Wanninkhof, R., 2007. Constraining global air-sea gas exchange for CO₂ with recent bomb ¹⁴C measurements. Glob. Biogeochem. Cycles 21, GB2015. http://dx.doi.org/10.1029/2006GB002784.

Takahashi, T., Olafsson, J., Goddard, J.G., Chipman, D.W., 1993. Seasonal variation of CO₂ and nutrients in the high-latitude surface oceans: a comparative study. Glob. Biogeochem. Cycles 7, 843–878.

Takahashi, T., Sutherland, S.C., Sweeney, C., Poisson, A., Metzl, N., Tilbrook, B., Bates, N., RikWanninkhof, R., Richard, A.F., Sabine, C., Olafsson, J., Nojiri, Y., 2002. Global sea–air CO₂ flux based on climatological surface ocean pCO₂, and seasonal biological and temperature effects. Deep-Sea Res. II 49, 1601–1622.

Takahashi, T., Sutherland, S.C., Wanninkhof, R., Sweeney, C., Feely, R.A., Chipman, D.W., Hales, B., Friederich, G., Chavez, F., Watson, A., Bakker, D.C.E., Schuster, U., Metzl, N., Yoshikawa-Inoue, H., Ishii, M., Midorikawa, T., Nojiri, Y., Sabine, C., Olafsson, J., Arnarson, Th.S., Tilbrook, B., Johannessen, T., Olsen, A., Richard, Bellerby, Körtzinger, A., Steinhoff, T., Hoppema, M., de Baar, H.J.W., Wong, C.S., Delille, Bruno, Bates, N.R., 2009. Climatological mean and decadal changes in surface ocean pCO₂, and net sea-air CO₂ flux over the global oceans. Deep-Sea Res. II 56, 554–577.

Ternon, J.F., Oudot, C., Dessier, A., Diverres, D., 2000. A seasonal tropical sink for atmospheric CO₂ in the Atlantic ocean: the role of the Amazon River discharge. Mar. Chem. 68, 183–201.

THERMO SCIENTIFIC CORPORATION, 2008. Solids Accessory, for Manual Introduction of Liquid Samples Containing Particles, Highly Viscous Samples and Solids. Chapter 1, General Information.

Tsunogai, S., Watanabe, S., Sato, T., 1999. Is there a "continental shelf pump" for the absorption of atmospheric CO₂? Tellus Ser. B 51, 701–712.

UNESCO, 1985. The international system of units (SI) in oceanography. UNESCO Technical Papers No. 45, IAPSO Pub. Sci. No. 32, Paris, France.

Vignudelli, S., Santinelli, C., Murru, E., Nannicini, L., Seritti, A., 2004. Distributions of dissolved organic carbon (DOC) and chromophoric dissolved organic matter (CDOM) in coastal waters of the northern Tyrrhenian Sea (Italy). Estuar. Coast. Shelf Sci. http://dx.doi.org/10.1016/j.ecss.2003.11.023.

Wanninkhof, R., 1992. Relationship between wind speed and gas exchange over the ocean. J. Geophys. Res. 97, 7373–7382.

Wanninkhof, R.H., 2014. Relationship between wind speed and gas exchange over the ocean revisited. Limnol. Oceanogr. Methods 12, 351–362.

Weiss, R.F., 1974. CO₂ in water and seawater: the solubility of a non-ideal gas. Mar. Chem. 2, 203–215.

Weiss, R.F., Price, B.A., 1980. Nitrous oxide solubility in water and seawater. Mar. Chem. 8, 347–359.